# Analysis of environmental isotopes in groundwater to understand the response of a vulnerable coastal aquifer to pumping: Western Port Basin, south-eastern Australia

Matthew Currell · Dioni I. Cendón · Xiang Cheng

**Abstract** The response of a multi-layered coastal aquifer in southeast Australia to decades of groundwater pumping, and the groundwater age, flow paths and salinization processes were examined using isotopic tracers. Groundwater radiocarbon and tritium contents decline with distance and depth away from basin margins; however, in the main zone of pumping, radiocarbon activities are generally homogeneous within a given depth horizon. A lack of tritium and low radiocarbon activities (<25pMC) in groundwater in and around the pumping areas indicate that seasonal recovery of water levels is related to capture of old water with low radioisotope activities, rather than arrival of recently recharged water. Mechanisms facilitating seasonal recovery include release of water from low-permeability layers and horizontal transfer of water from undeveloped parts of the basin. Overall stability in seasonally recovered water levels and salinities for the past three decades indicate that the system has reached a dynamic equilibrium with respect to water balance and salinity, following a major change in flow paths and solute distributions after initial development. Groundwater $\delta^{18}O$, $\delta^{2}H$ and chloride contents indicate mixing between fresh meteoric-derived groundwater and marine water at the coast, with the most saline groundwater approximating an 80:20 mixture of fresh to oceanic water.

Received: 10 January 2013 / Accepted: 18 June 2013
Published online: 18 July 2013



M. Currell (✉)
School of Civil, Environmental and Chemical Engineering,
RMIT University, GPO Box 2476, Melbourne, VIC 3001, Australia
e-mail: matthew.currell@rmit.edu.au
Tel.: +61-3-99250402

D. I. Cendón
Australian Nuclear Science and Technology Organisation,
Locked Bag 2001, Kirrawee, NSW 2232, Australia

D. I. Cendón
School of Biological and Environmental Sciences,
The University of New South Wales, Sydney, NSW 2052, Australia

X. Cheng
Department of Primary Industries, Parkville, VIC 3010, Australia

**Keywords** Groundwater age · Australia · Environmental isotopes · Salinization · Coastal aquifers

## Introduction

With over half of the world's population living within 200 km of oceans, freshwater coastal aquifers are some of the most important and vulnerable water resources globally. Increasing water demand and the threat of rising sea levels are intensifying pressure on coastal aquifers and increasing the potential for saline intrusion (e.g., Werner and Simmons 2009; Barlow and Reichard 2010). Hence, extensive work has gone into conceptualizing and modelling modes of seawater intrusion, and developing vulnerability and risk assessment methods (e.g. Strack 1976; Post and Abarca 2010; Carrera et al. 2010; Været et al. 2012; Werner et al. 2012). While systems with a well-defined saltwater wedge, well-constrained aquifer geometry and known physical parameters can be modelled and monitored using simple field tools, there are many cases in which hydrogeological conditions create complex modes of salinization (e.g. Vengosh et al. 2005; Mulligan et al. 2007). In such cases geochemical tracers, including radiogenic and stable isotopes, offer an ability to improve conceptual models of flow, water balance and controls on water quality (e.g. Vengosh et al. 2002, 2005; Andersen et al. 2005; Gattacceca et al. 2009). In this study, geochemical tools, including stable isotopes of water, age dating tracers and major ions, are used to aid conceptualization of a vulnerable coastal aquifer (Western Port Basin in south-eastern Australia), in which the distribution of groundwater salinity cannot be explained in terms of a classic saltwater/freshwater interface. The tracer data are also used as new lines of evidence with which existing notions about the water balance, including the response to groundwater extraction, are re-assessed.

The Western Port Basin is located approximately 70 km southeast of the city of Melbourne, Australia, and hosts an aquifer system that provides water supply for agriculture, stock and domestic use (Fig. 1). Due to its proximity to a major urban centre, the study area and similar aquifers are increasingly seen as important for maintaining sustainable, locally based food sources for growing urban populations. Because of the relatively small size and proximity to the

 DOI 10.1007/s10040-013-1017-9

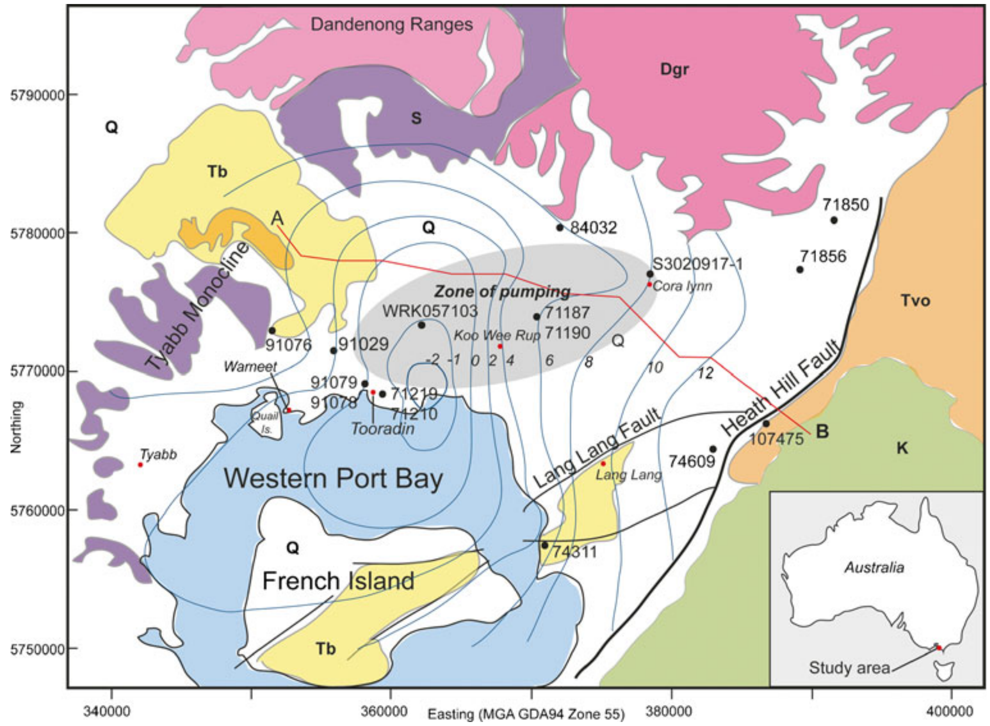


**Fig. 1** Simplified geological map of the study area and sample locations. Surface geological units: *Q* (Quaternary); *Tb* (Baxter Formation); *Tvo* (Older Volcanics); *K* (Strzelecki Group); *Dgr* (Devonian granite); *S* (Silurian mudstone). Further details of units are provided in Fig. 3. Sample locations are shown as *black dots* with bore ID within the State Observation Bore Network of Victoria. Potentiometric head contours (in metres relative to Australian Height Datum; *blue lines*) in the Western Port Group aquifer are shown as of June 2011. *A–B* is the cross section in Fig. 2. *Red dots* are towns

coast, it is considered to be vulnerable, and has been designated as a water-supply protection area (WSPA) under State legislation. The region is facing increasing pressure from encroaching urban development and climatic variability—experiencing an extended drought through the first decade of the 2000s, while continuing to supply water for irrigation and domestic use.

Previous hydrogeological investigations have been carried out by means of drilling and groundwater monitoring programs (Lakey and Tickell 1980, 1981), numerical modelling (Longley et al. 1978; Cheng 1999), and water-quality assessments (Carrillo-Rivera 1975; Cheng 1999; SKM 2003). However, there remain a number of outstanding questions, which are of broad interest to general discussions regarding sustainable utilization of groundwater (e.g. Alley et al. 1999; Bredehoeft 2002). Of particular interest is better understanding the nature of the aquifer's dynamic response to seasonal pumping, and the mechanism by which seasonal recovery of water levels occurs (e.g. arrival of recent recharge in the zone of pumping, versus transfer of older water from storage elsewhere in the basin). The timescales of recharge, through-flow and discharge are also poorly understood, although estimates have been made on purely physical/modelling approaches, without any comparison with tracer data (Longley et al. 1978; Lakey and Tickell 1980; SKM 2003). Finally, water-quality and salinization mechanisms are of interest, particularly in the context of extensive groundwater abstraction. In the past, sources of salinity and mechanisms of groundwater salinization have been proposed, but these have not been assessed using isotope tracers. The geochemical data collected for this study provide new evidence with which these issues are explored. The primary objectives are: (1) to use radiogenic isotopes to constrain the spatial distribution of groundwater ages and better define flow systems in the Western Port Basin; (2) determine the mechanism(s) by which water levels in the zone of groundwater pumping recover following the cessation of pumping each year; (3) to understand the sources of salinity in groundwater and re-assess a previously proposed mechanism by which marine water is incorporated into the aquifer at the coast (Lakey and Tickell 1980).

## Hydrogeology of the Western Port Basin

The Western Port Basin occupies a fault-bounded sunkland extending ~30 km in the east–west and ~50 km in the north–south direction (Fig. 1). The basin contains a sequence of sediments and volcanic rocks, mostly deposited during the Cainozoic, which reach a maximum thickness of 300 m in the southeast (Fig. 2 and Fig. 3). Underlying and adjacent to the Cainozoic sediments are basement rocks consisting of Devonian granite to the northeast, Silurian mudstone and sandstone to the northwest and west, and Lower Cretaceous sandstone and mudstone to the east and southeast (Carrillo-Rivera 1975; Fig. 1). The major structural boundaries are the north–north-easterly trending Heath Hill fault (eastern margin), Tyabb monocline (western margin) and the Dandenong Ranges (northern margin). To the south, the basin sediments

 DOI 10.1007/s10040-013-1017-9

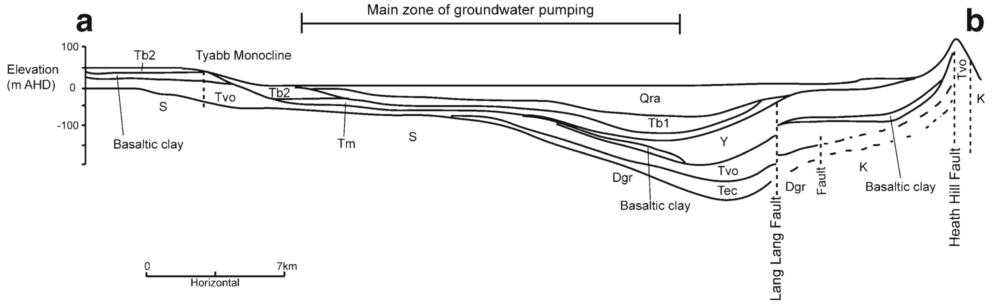


**Fig. 2** Simplified geological cross section across Western Port Basin (modified from Cheng 1999 and Lakey and Tickell 1980). *Unit symbols* are as described in Fig. 1 and Fig. 3; location of section shown in Fig. 1

continue below Western Port Bay—a shallow marine embayment, outcropping on French Island where they thin above the faulted, uplifted basement below the island. Within the bay, the depth to the ocean floor is generally shallow (<5 m), however, it is deeper within the tidal-channel (in places up to 30 m), which may represent a drowned fluvial system, active during periods of lower sea-level. Sediments in the bay to the north of French Island are predominantly silt and clay, with areas of sandy sediment confined to the tidal channel, particularly the western arm (Rosengren 1984). Prior to European settlement in the 19th century, the onshore area was mostly covered by swampland (‘The Great Swamp’), which was gradually drained through the 19th and early 20th centuries by a canal network.

The majority of water-supply bores extract groundwater from the Cainozoic Western Port Group, comprising three major units—the fluviatile iron-rich sands and sandy clays of the Baxter Formation; the transitional-to-marine carbonaceous sands, marl and limestone of the Sherwood Formation; and the coarse gravels, clays and minor coals of the Yallock Formation (Fig. 3). These are overlain by Quaternary swamp (and locally, dune) deposits, which may act as confining layers, except at the Basin margins, where the older sediments are present near the surface (Fig. 1). The other major unit from which groundwater is extracted is the Older Volcanics, which underlie the Western Port Group, comprising fractured basalt deposited in sheet flows, locally separated by volcanic clays, pyroclastics and other thin sedimentary horizons (Fig. 2). High yields of good quality groundwater can also be obtained from the underlying Childers Formation (coarse, silica-rich fluvial sediments); however, drilling costs and the availability of shallower groundwater have limited development of this unit to date.

## Groundwater extraction

The Basin was one of the first aquifer systems in southeast Australia to have been developed for water supply, beginning in the 1920s (Southern Rural Water 2010). At this time, aquifer pressures were artesian and the groundwater flow direction southward, towards Western Port Bay (Threader 1952). Groundwater development expanded rapidly in the 1950s and 60s to support irrigated production of vegetables. Following this, a cone of depression developed surrounding the townships of Koo Wee Rup and Cora Lynn, where aquifer pressures declined below sea level over an area of ~150 km$^2$. In response to high levels of groundwater extraction, and fears over seawater intrusion, the area was declared a Groundwater Conservation Area in 1971. Currently groundwater usage is controlled by licensing, metering and caps on extractions. Pumping from the Western Port Group and Older Volcanics is highly seasonal (mostly between October and March), and potentiometric pressures in these units exhibit seasonal decline and recovery, synchronous with periods of extraction and non-extraction. While there was an overall decline in aquifer pressures after development of the resource, eliminating artesian conditions, pressures have largely stabilised, excluding short-term rises and falls associated with seasonal pumping. It has been generally assumed that long-term stability of aquifer pressures and seasonal recovery of water levels are indicative of a system in which discharge through extraction is approximately equalled by recharge (e.g. Southern Rural Water 2010). However, this assumption has not been interrogated, nor have the specific sources of capture and dynamic response of the aquifer to pumping been assessed in detail, until this study.

## Water quality

Water-quality analyses have been conducted sporadically over the last 30–40 years from a network of observation bores. Carrillo-Rivera (1975) presented the first analysis of hydrochemical data, including major ions and the halogens I and Br, which were analysed as potential indicators of trapped seawater in the basin. Subsequent analyses of EC, pH, major ions and trace elements were conducted at varying frequencies over the last 30 years (e.g. SKM 1997). The spatial distribution of water quality is variable both horizontally and vertically across the basin (Lakey and Tickell 1981). The most saline groundwater is found immediately adjacent to the coast of Western Port Bay (near Warneet and Tooradin), while there are also inland saline water bodies in the western and northern parts of the basin. Trends in groundwater EC over time indicate that there has been little upward or downward trend in average salinities (including coastal bores) since regular monitoring began in the mid-1980s (Fig. 4). However, there was an increase in salinities observed in a number of parts of the basin immediately following the

 DOI 10.1007/s10040-013-1017-9

| Age | | Stratigraphy | | | Lithology and depositional environment | Aquifer types and form | Bore yield | Typical hydraulic conductivity (m/day) | Storage coefficient (× $10^{-3}$) |
|---|---|---|---|---|---|---|---|---|---|
| Cainozoic | Quaternary | | | | Sand, medium to coarse quartzose; aeolian deposition. | Unconfined sand aquifer, sheet-like form with limited distribution. | Up to 2.5 L/s | | |
| | | | | Qra | Clay, minor felspathic shoestring sand and gravel. Fluvial deposition. | Unconfined to semi-confined aquifer of sand and gravel. Shoestring type form. Interbedded in clay. Generally of low hydraulic conductivity. | Up to 10 L/s (mostly lower) | | |
| | Miocene | Western Port Group | Baxter Formation | Tb2 | Sand, medium to coarse, quartzose, gravel; often carbonaceous, numerous lignite and carbonaceous caly beds; fluvial and paludal deposition. | Unconfined to confined aquifer of unconsolidated sand and gravel, sheet-like form; beds of clay, lignite and cemented limestone impart marked anisotropy in hydraulic conductivity. Clayey soil up to 5m thick partially confines the groundwater. | Up to 25 L/s. | 2.5–4.0 | 0.3–30 |
| | | | | Tb1 | Sand, fine; transitional from littoral marine to fluvial deposition. | | | 1.0–2.6 | 0.2 |
| | Oligocene | | Sherwood Formation | Tm | Sand, fine to medium, calcareous, often silty; minor limestone; shallow marine deposition. | | | 1.0–1.3 | 0.2 |
| | | | | Tml | Calcarenite with sand, silt and clay matrix; shallow marine deposition. | | | 2.4–8.5 | 0.25 |
| | | | Yallock Formation | Y | Sand, medium to coarse quartzose; gravel, often carbonaceous; minor lignite; fluvial and paludal deposition. | | | 3.0–4.8 | 0.3–350 |
| | Eocene | Older Volcanics | | Tvo | Clay; highly weathered basalt. | Aquitard to aquiclude, discontinuous, where present restricts upward leakage from the underlying fresh basalt and Childers Formation aquifers. | | | |
| | | | | | Basalt. | Semi-confined to confined aquifer, sheet-like form. Hydraulic conductivity varies according to development of secondary porosity. | Up to 15L/s | 2.9–11.7 | 0.5–5 |
| | | Childers Formation | | Tec | Sand, coarse quartzose; gravel; often carbonaceous, numerous lignite and hard carbonaceous clay beds, fluvial and paludal deposition. | Semi-confined to confined aquifer of sand and gravel, sheet-like form; lignite and clay beds impart marked anisotropy in hydraulic conductivity. | 2.5-25L/s | 3.0–3.7 | 0.25–8 |
| Mesozoic | Cretaceous | Strzelecki Group | | K | Sandstone, felspathic siltstone, mudstone. | | | | |
| Palaeozoic (lower) | | | | | Granite, granodiorite. Mudstone, siltstone, sandstone. | Little known, but includes some minor fractured rock aquifers. | | | |

**Fig. 3** A summary of geology and hydrogeology in Western Port Basin (adapted from Lakey and Tickell, 1981)


DOI 10.1007/s10040-013-1017-9

**Table 1** Groundwater hydrochemical analyses and site location data

| Bore ID | Date sampled | [a]Easting | Northing | Unit | Screen (m) from | to | EC (μS/cm) | pH | Dissolved oxygen (mg/L) | Na[b] | Mg | K | Ca | Cl | Br | $NO_3$ | $SO_4$ | $HCO_3$ | $\delta^2H$ (‰) | $\delta^{18}O$ (‰) |
|---|---|---|---|---|---|---|---|---|---|---|---|---|---|---|---|---|---|---|---|---|
| 71219 | 9.9.11 | 358886 | 5768832 | Baxter | −21 | −39 | 12,200 | 6.42 | 0.34 | 93.18 | 16.85 | 1.78 | 8.68 | 96.9 | 0.14 | 0.06 | 5.55 | 8.40 | −30.3 | −4.4 |
| 71219 | 16.1.12 | 358886 | 5768832 | Baxter | −21 | −39 | 13,350 | 6.74 | 0.5 | 120.00 | 16.47 | 2.60 | 7.50 | 109 | 0.16 | 0.20 | 6.61 | 8.18 | −29.7 | −4.5 |
| 71216 | 10.9.11 | 357999 | 5768906 | Baxter | −27 | −33 | 8,220 | 7.15 | ND | 45.52 | 8.11 | 0.39 | 7.36 | 62.2 | 0.10 | 0.06 | 0.88 | 4.96 | −29.6 | −4.4 |
| 91076 | 26.1.12 | 351069 | 5773317 | Baxter | −12 | −18 | 11,230 | 6.42 | 0.95 | 95.65 | 24.34 | 1.14 | 4.08 | 100 | 0.12 | 0.05 | 2.04 | 3.72 | −29.9 | −4.6 |
| 91079 | 11.11.11 | 357573 | 5769467 | Baxter | −30 | −33 | 8,750 | 6.2 | 0.25 | 50.98 | 10.00 | 0.26 | 6.75 | 69.5 | 0.09 | 0.05 | 1.20 | 3.78 | −30.3 | −4.5 |
| 91079 | 17.1.12 | 357573 | 5769467 | Baxter | −30 | −33 | 8,560 | 6.34 | 1 | 69.48 | 11.42 | 0.82 | 6.76 | 68.8 | 0.10 | 0.01 | 1.17 | 3.80 | −29.0 | −4.9 |
| 74311 | 10.9.11 | 370320 | 5757943 | Baxter | −18 | −25 | 1,000 | 5.9 | 0.6 | 5.30 | 0.84 | 0.09 | 0.30 | 6.82 | 0.01 | 0.01 | 0.04 | 0.68 | −32.1 | −5.0 |
| 74311 | 26.02.12 | 370320 | 5757943 | Baxter | −18 | −25 | 990 | 5.85 | 0.45 | 6.66 | 1.03 | 0.31 | 0.53 | 6.95 | 0.01 | 0.02 | 0.04 | 1.14 | −31.2 | −5.3 |
| 71210 | 9.9.11 | 358894 | 5768835 | Sherwood | −51 | −62 | 5,100 | 7.1 | 0.3 | 35.97 | 6.62 | 0.78 | 3.69 | 38.0 | 0.06 | 0.02 | 2.05 | 4.70 | −33.2 | −5.2 |
| 71210 | 16.1.12 | 358894 | 5768835 | Sherwood | −51 | −62 | 3,440 | 7.93 | 0.55 | 29.52 | 4.86 | 0.90 | 2.90 | 25.5 | 0.04 | 0.05 | 0.43 | 5.28 | −32.3 | −5.5 |
| 91029 | 10.9.11 | 355372 | 5772091 | Sherwood | −36 | −59 | 1,900 | 8.4 | 0.13 | 9.67 | 1.55 | 0.12 | 2.26 | 12.1 | 0.01 | 0.01 | 0.00 | 2.28 | −34.3 | −5.1 |
| 91029 | 19.1.12 | 355372 | 5772091 | Sherwood | −36 | −59 | 2,115 | 7.81 | 0.5 | 11.86 | 1.79 | 0.11 | 3.95 | 13.9 | 0.02 | 0.02 | 0.21 | 4.72 | −33.1 | −5.4 |
| 91078 | 17.1.12 | 357574 | 5769462 | Sherwood | −72 | −92 | 5,600 | 8.27 | 1.3 | 44.30 | 7.50 | 0.57 | 2.15 | 45.8 | 0.06 | 0.02 | 0.03 | 0.48 | −31.7 | −5.4 |
| 71190 | 9.9.11 | 369855 | 5774539 | Sherwood | −41 | −49 | 2,540 | 6.79 | ND | 14.13 | 4.11 | 0.21 | 1.40 | 19.5 | 0.02 | 0.00 | 0.02 | 2.80 | −29.4 | −4.5 |
| 71190 | 16.1.12 | 369855 | 5774539 | Sherwood | −41 | −49 | 2,960 | 7.22 | 0.44 | 15.77 | 3.66 | 0.16 | 1.15 | 21.0 | 0.02 | 0.01 | 0.01 | 3.80 | −29.9 | −4.8 |
| 71856 | 19.1.12 | 388764 | 5777656 | Sherwood | −75 | −88 | 4,070 | 8.75 | 0.85 | 30.80 | 6.14 | 0.47 | 1.42 | 31.6 | 0.04 | 0.01 | 0.45 | 4.40 | −32.9 | −5.5 |
| S9020317-1 | 26.01.12 | 377956 | 5777206 | Yallock | −51 | −81 | 2,790 | 6.14 | 0.46 | 18.04 | 3.80 | 0.25 | 1.57 | 20.9 | 0.03 | 0.01 | 0.20 | 2.94 | −33.5 | −5.5 |
| 71850 | 19.1.12 | 391459 | 5781379 | Yallock | −44 | −52 | 4,030 | 6.48 | 1.5 | 30.39 | 5.21 | 0.60 | 0.70 | 30.4 | 0.04 | 0.01 | 0.13 | 2.74 | −32.0 | −5.4 |
| 145259 | 10.9.11 | 379226 | 5761228 | Yallock | −37 | −40 | 455 | 6.45 | 0.25 | 1.75 | 0.28 | 0.04 | 0.93 | 1.82 | 0.00 | 0.00 | 0.13 | 1.68 | −32.9 | −5.1 |
| 74609 | 11.11.11 | 382543 | 5764751 | Yallock | −20 | −35 | 400 | 6.3 | 0.5 | 1.92 | 0.22 | 0.03 | 0.02 | 2.00 | 0.00 | 0.00 | 0.00 | 1.36 | −33.6 | −5.2 |
| 74609 | 19.1.12 | 382543 | 5764751 | Yallock | −20 | −35 | 395 | 6.49 | 0.35 | 1.97 | 0.24 | 0.01 | 0.00 | 2.06 | 0.00 | 0.00 | 0.01 | 1.42 | −33.6 | −5.7 |
| WRK057103 | 16.1.12 | 361879 | 5773524 | Older Volcanics | −70 | −73 | 2,130 | 7.61 | 0.6 | 13.20 | 2.52 | 1.18 | 2.62 | 12.5 | 0.02 | 0.03 | 0.00 | 6.94 | −33.3 | −5.7 |
| 71187 | 16.1.12 | 369850 | 5774542 | Older Volcanics | −68 | −73 | 2,320 | 7.68 | 0.64 | 15.63 | 2.91 | 0.28 | 2.23 | 15.3 | 0.02 | 0.01 | 0.03 | 6.08 | −34.1 | −5.5 |
| 84032 | 17.1.12 | 371770 | 5780933 | Older Volcanics | −48 | −60 | 8,460 | 6.8 | 0.6 | 81.70 | 11.13 | 0.44 | 2.06 | 67.7 | 0.09 | 0.01 | 2.37 | 3.98 | −33.5 | −5.0 |
| 107475 | 26.01.12 | 386150 | 5766374 | Older Volcanics | −19 | −21 | 2,280 | 6.57 | 0.45 | 12.93 | 3.50 | 0.11 | 1.78 | 18.3 | 0.02 | 0.00 | 0.27 | 3.48 | −30.3 | −5.2 |

[a] Map Grid of Australia (GDA 1994) Zone 55, *ND* not detected
[b] All ion concentrations are in units of mmol/L


DOI 10.1007/s10040-013-1017-9

**Table 2** Radioisotope data from groundwater

| Sample code[a] | Bore ID[b] | Distance from coast (km) | Geological Unit | Depth (screen midpoint) | Tritium (TU)[c] | $^{14}$C (pMC) | $\delta^{13}$C (‰) | Age (Uncorrected) | Calcite saturation index |
|---|---|---|---|---|---|---|---|---|---|
| OZO861 | 71219 | 0.5 | Baxter | −30 | 0.03 | 23.91 | −18.4 | 11,490 | −0.14 |
| OZO856 | 91076 | 4.5 | Baxter | −15 | 0.23 | 73.17 | −16.3 | 2510 | −1.04 |
| OZO865 | 91029 | 2.9 | Sherwood | −47.5 | 0.02 | 0.91 | −12.4 | 37,790 | 0.75 |
| OZO862 | 71210 | 0.5 | Sherwood | −56.5 | 0.01 | 3.09 | −17.2 | 27,930 | −0.65 |
| OZO859 | 71190 | 7.8 | Sherwood | −45 | 0.02 | 21.09 | −10.6 | 12,500 | −0.46 |
| OZO867 | 71856 | 23.5 | Sherwood | −81.5 | 0.01 | 4.99 | −21.9 | 24,080 | 1.03 |
| OZO864 | 91078 | 0.5 | Sherwood | −77 | 0.02 | 24.95 | 18.2 | 11,150 | −0.19 |
| OZO866 | S9020317-1 | 14.2 | Yallock | −66 | 0.08 | 6.59 | −18.2 | 21,850 | −1.55 |
| OZO869 | 71850 | 23.7 | Yallock | −48 | 0.01 | 21.77 | −19 | 12,250 | −1.64 |
| OZO858 | 74311 | 0.05 | Yallock | −21 | 0.04 | 48.53 | −17.8 | 5,810 | −2.58 |
| OZO868 | 74609 | 14.1 | Yallock | −27.5 | 0.1 | 61.15 | −15.5 | 3,950 | −3.02 |
| OZO870 | WRK057103 | 5.2 | Older Volcanics | −71.5 | 0.05 | 1.39 | −17.2 | 34,350 | 0.54 |
| OZO863 | 71187 | 7.8 | Older Volcanics | −70.5 | 0.01 | 0.99 | −21.3 | 37,040 | 0.46 |
| OZO860 | 84032 | 14.5 | Older Volcanics | −54 | 0.01 | 6.27 | −16.3 | 22,250 | −0.81 |
| OZO857 | 107475 | 16.5 | Older Volcanics | −20 | 0.09 | 78.77 | −19.6 | 1,915 | −0.96 |

[a] ANSTO code

[b] Identifier code for Victorian State Observation Bore Network

[c] Minimum quantification limit=0.15 TU

drought and major increase in bore development in 1967 (Carrillo-Rivera 1975).

## Methods

Groundwater samples were collected in September 2011 and January 2012 from observation bores, which are regularly monitored as part of the Victorian State Observation Bore Network. Bores were chosen on the basis of spatial coverage, with transects selected to include the coast, pumping zone and basin margins. Bores with narrow screen intervals were favoured to capture water from discreet sections of the aquifer (Table 1). Sampling was carried out using a piston pump (Bennet pump) operated at low flow rates (~0.05 L/s); both drawdown and physico–chemical parameters (EC, pH and dissolved oxygen) were allowed to stabilize prior to collection of the samples in pre-conditioned HDPE bottles. Samples for major cation analysis were filtered (0.45-µm cellulose acetate) and acidified in the field with concentrated, double-distilled $HNO_3$. Stable isotopes of water and major ions were analysed at the Monash University School of Geosciences, using IRMS, IC and ICP-MS, following methods described in Cartwright et al. (2010).

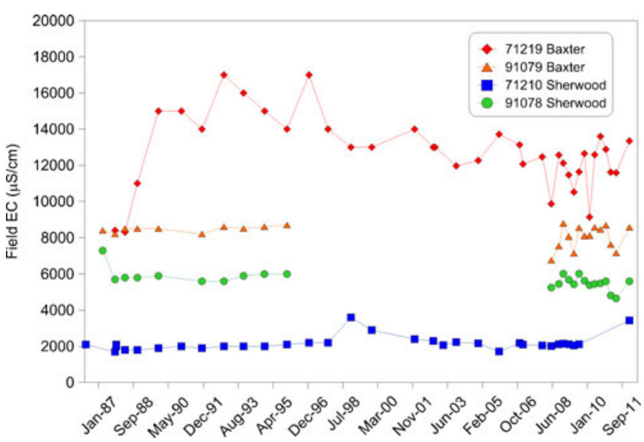


**Fig. 4** Time series of electrical conductivity (*EC*) from selected coastal bores in the study area; sites shown on Fig. 1 (data from Victoria Water Data Warehouse). Bore screen interval and location details are included in Table 1

Samples for carbon-14 and tritium analysis were collected in 1 and 2-L HDPE bottles, filled by displacing air from the base of the bottle upwards and capping while submerged in a bucket full of the flowing groundwater, to minimize contact with the atmosphere. These samples were analysed at the Australian Nuclear Science and Technology Organisation. For $^3$H, samples were distilled and enriched via electrolysis before being analysed using liquid scintillation counting. The concentrations are expressed as tritium units (TU), and have 1σ uncertainties between 0.01 and 0.03, with a minimum quantification limit of 0.15 TU (Table 2). For $^{14}$C, dissolved inorganic carbon (DIC) was liberated from the filtered samples with phosphoric acid as $CO_2$, which was captured using a custom-built extraction line. The $CO_2$ samples were heated in sealed glass tubes containing baked CuO, and Ag and Cu wire for 2 h at 600 °C to remove sulfur compounds liberated by this process. The $CO_2$ was then converted to graphite by reduction with hydrogen gas in the presence of an iron catalyst, still at 600 °C. Activities of $^{14}$C were measured on graphite targets by accelerator mass spectrometry using the ANSTO 2MV tandetron accelerator STAR (Fink et al. 2004), and reported as percent Modern Carbon (pMC), with a range of 1σ errors between ±0.03 and 0.4. Radiocarbon age calculations were performed following methods outlined in Stuiver and Polach (1977). The uncorrected ages quoted are ‘conventional radiocarbon ages’ (years Before Present) rather than calendar ages, and use a half-life of 5,568 years. All $^{14}$C measurements were normalized against the oxalic acid (HOXI) international standard. The method assumes that atmospheric $^{14}$C levels have been constant in the past, and

 DOI 10.1007/s10040-013-1017-9

that isotopic fractionation of all sample activities is accounted for by normalizing $\delta^{13}C$ to −25 ‰ relative to PDB. PHREEQC (version 2.4, Parkhurst and Appelo 1999) was used to calculate saturation indices of the water with respect to calcite (Table 2). The $\delta^{13}C$ values of DIC in groundwater were also measured at ANSTO on the graphite targets, using EA-IRMS. A subset of the water samples were also analysed independently for $\delta^{13}C$ using IRMS at Monash University, using the method described in Cartwright et al. (2010). The resulting $\delta^{13}C$ values from the two methods were consistent, plotting on a straight line with 1:1 slope.

## Results

### Tritium and radiocarbon

Only one sample, from a relatively shallow bore (91076; screened from −12 to −18 m), contained tritium above the minimum quantification limit of 0.15 TU, indicating any significant input of modern water. In this case 'modern' is defined as the last ~50 years, since the global peak in atmospheric nuclear testing (1962–1963). The current concentration of tritium in precipitation from the southern hemisphere is at natural background levels, ~2 TU (cf. Morgentern et al. 2010). Peak tritium concentrations in rainfall measured for Melbourne during 1963 ranged between 30 and 105 TU (Calf 1988); by 2012 tritium in this water would be expected to have decayed to ~1.5–6.5 TU and thus still be measurable in groundwater recharged at this time. Rainfall concentrations above ~10 TU were still commonly recorded up until the early 1980s, meaning water recharged at this time would also still contain measurable tritium (>1.5 TU). Any subsequent recharge, while containing lower initial concentrations, would still be expected to contain at least ~0.5 TU. Hence, water recharged since ca. 1962 would be expected to contain measurable tritium, unless substantial loss has occurred by mechanisms other than decay (e.g. diffusion to dead-end pores).

Radiocarbon percent Modern Carbon values in groundwater range from 0.99 to 78.8 pMC. Uncorrected ages, which should be interpreted as broad, provisional estimates of the mean ages of groundwater sampled at these points, range between 1,900 and >30,000 years BP (Table 2). The majority of samples in the Western Port Group and Older Volcanics exhibit ages corresponding to recharge during the late Pleistocene. A decrease in $^{14}C$ values with depth is observed throughout the basin (Fig. 5), while along the two transects of bores (labelled 'transect 1' and 'transect 2'), the $^{14}C$ values follow a weak trend of declining with distance from the basin margins towards the coast (Fig. 6). These data are consistent with a system in which recharge occurs at the basin margins, with subsequent groundwater flow, over millennial timescales, towards the central and southern parts of the basin. However, there is generally greater difference in the $^{14}C$ values between units in the vertical dimension than between horizontal locations in an aquifer unit. The horizontal decline in tracer activities away from the basin margin is more pronounced in transect 2 (see Fig. 6), suggesting that conventional horizontal flow towards the coast is more important in this area, which is largely unaffected by groundwater pumping.

Dissolved inorganic carbon may be derived from a variety of sources, including dissolution of soil gas $CO_2$ during recharge; oxidation of aquifer organic carbon; and dissolution or exchange with aquifer carbonate minerals. The optimal correction model(s) to be employed to account for dissolution or exchange with $^{14}C$-free aquifer carbon has been longstanding topic of conjecture (Fontes and Garnier 1979; Clark and Fritz 1997; Coetsiers and Walraevens 2009; Gillon et al. 2009; Han et al. 2012). In the Western Port Basin, the main sources of potential dead carbon are decomposition of organic matter, particularly coal and lignite in the Western Port Group, and marine carbonate in the Sherwood Formation. The $\delta^{13}C$ values in groundwater range from −10.6 to −21.9 ‰; samples from bores 71190 and 91029, screened in the upper Sherwood Formation, contain the highest values (−10.6 and −12.4 ‰ respectively), indicating a component of marine carbonate. The remaining samples have $\delta^{13}C$ values between −15.5 and −21.9 ‰, with most samples (e.g. 71187, 71856, 71850) showing more depleted $\delta^{13}C$ than those expected for silica-rich sedimentary formations (e.g. Meredith et al. 2012). This could be accounted for by the incorporation of $HCO_3$ from decay of old organic matter (with $\delta^{13}C$

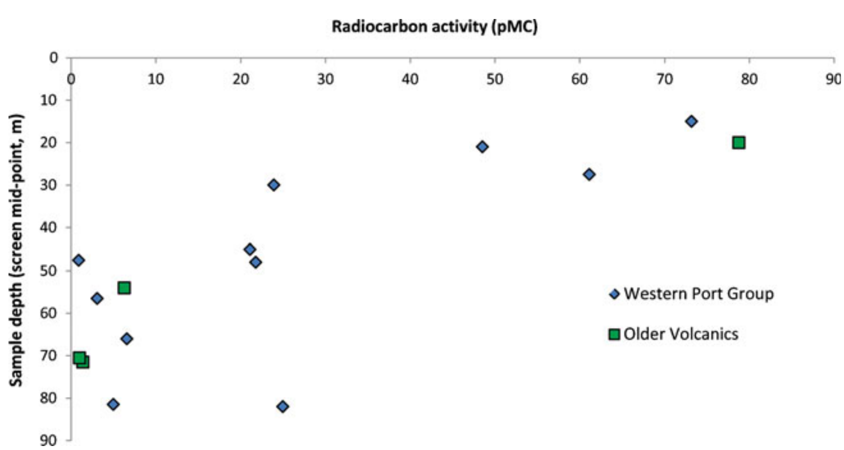


**Fig. 5** Radiocarbon activity (*pMC*) of groundwater versus depth in the *Western Port Group* and *Older Volcanics*

 DOI 10.1007/s10040-013-1017-9

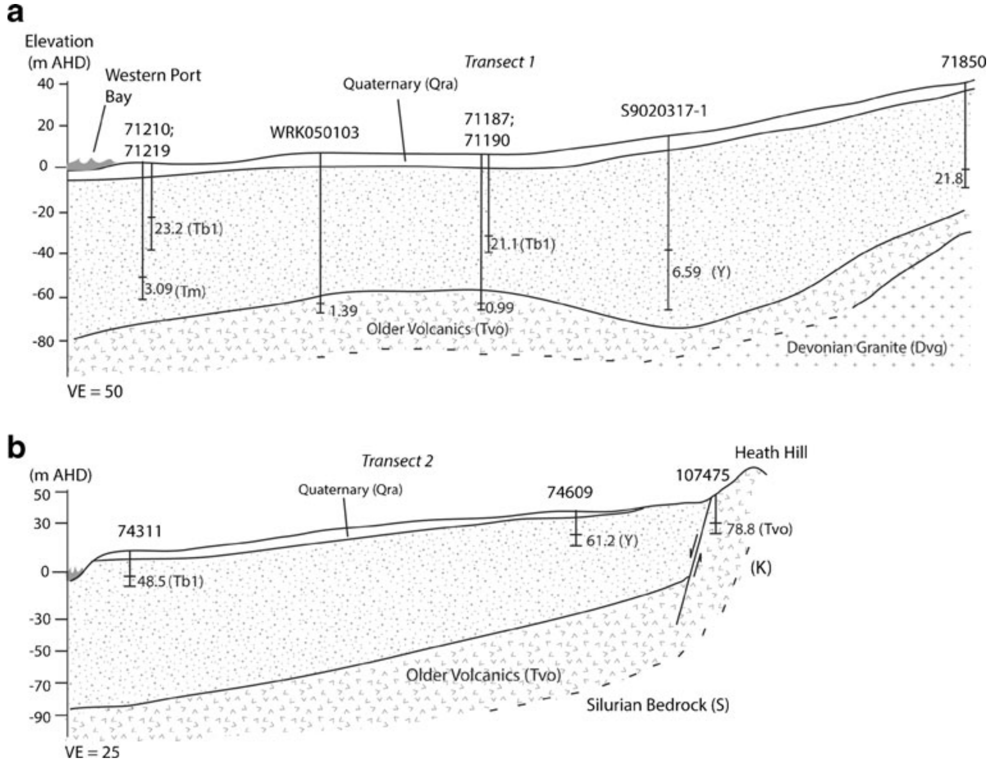


**Fig. 6** Transects of sampled bores, showing radiocarbon activity (pMC) at each sample point (see Fig. 1 for locations). Screened intervals of each sampled bore are indicated, with $^{14}C$ (pMC) values and geological unit indicated next to the interval (refer to Fig. 3 for geological unit key)

values on the order of ~−25 ‰). In most groundwater with salinities <5,000 mg/L, there is a moderate positive correlation between $HCO_3$ and Ca ($R^2$=0.4), which suggests calcite dissolution; however, there is no correlation between the DIC concentrations and $\delta^{13}C$ values, as would be expected if this was a dominant source of carbon. Overall, the typical contribution of matrix carbon to groundwater in minor carbonate and coal-bearing sediments and basalts is ~15–35 % (e.g. Clark and Fritz 1997), which would mean that the uncorrected ages may overestimate the mean groundwater age in each sample by approximately this amount.

Notwithstanding the potential influence of aquifer-derived carbon on the age estimates, the absence of tritium and low radiocarbon activities observed in much of the basin point to the fact that much of the water in the area where groundwater extraction occurs was recharged thousands, or tens of thousands of years before present (between the mid-Holocene and late Pleistocene). The past hydrological and climatic regime—including variations in sea level, would thus have influenced the present-day groundwater heads and solute distributions (e.g. Været et al. 2012). A more detailed discussion of the geological and geomorphological history and its relationship to the groundwater recharge history is however beyond the scope of this report.

## Stable isotopes

The groundwater $\delta^{18}O$ and $\delta^2H$ compositions range from −4.4 to −5.7 ‰ and −29.6 to −34.3 ‰, respectively (Table 1). Cheng (1999) also reported stable isotope data from samples collected in 1997, which exhibited similar, although in some cases slightly lower $\delta^{18}O$ and $\delta^2H$ compositions (range: −4.5 to −5.5 ‰ and −30 to −39 ‰, respectively). Most samples plot close to or slightly to the right of the local meteoric water line (LMWL; Fig. 7). Deviation from the LMWL is greatest for saline groundwater in the Western Port Group, sampled near the coast. The $\delta^{18}O$ and Cl values show a positive correlation ($R^2$=0.45), and a pattern that is commensurate with mixing between a fresh rainfall derived end-member with $\delta^{18}O$ between −5.0 and −6.0 ‰ and Cl

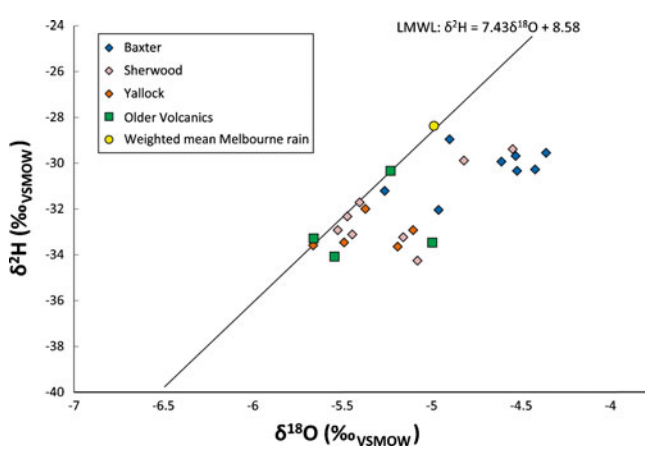


**Fig. 7** Stable isotope compositions of samples with geological units indicated, and local meteoric water line (data from IAEA-WMO Global Network for Isotopes in Precipitation; Local Meteoric Water Line calculated according to method of Hughes and Crawford 2012)


DOI 10.1007/s10040-013-1017-9

concentration of 0.06 mmol/L (Herczeg and Edmunds 2000), and a saline, oceanic end-member with $\delta^{18}O$ of 0.0 ‰, and Cl concentration (cf. Millero 1996) of 545.8 mmol/L (Fig. 8). Taking into account the influence of this mixing, the majority of groundwater appears to have started out with lower $\delta^{18}O$ and $\delta^{2}H$ values than the current weighted mean composition of rainwater from Melbourne (−4.98, −28.4 ‰). This indicates that groundwater was recharged by rainfall or surface water with slightly more depleted isotope compositions than modern rainfall. There is no noticeable trend in the stable isotope compositions across the spectrum of measured radiocarbon activities to suggest a shift in stable isotope compositions relating to long-term climatic change (e.g., Jiráková et al. 2011). However, this cannot be ruled out entirely—a broad shift in rainwater stable isotope compositions over the late Pleistocene and Holocene periods in southern Australia was observed in confined groundwater in the Otway Basin, located at similar latitude (Love et al. 1994).

Bores sampled during both sampling rounds showed broadly consistent stable isotope compositions (Table 1); indicating that overall the sources of water are consistent on yearly/seasonal timescales; however, small variations were observed in some of the bores between sampling rounds, suggesting variation in the proportions of different water sources arriving at the wells during the pumping and non-pumping seasons, e.g., water from higher/lower permeability layers, or marine water. In general, the isotope compositions tend to be more depleted in the September sampling (non-pumping season) than the January sampling (pumping season), by about 0.5 ‰ for $\delta^{18}O$.

## Discussion

### Recharge sources and flow paths

Proposed sources of recharge to the aquifer system include: (1) Recharge along the Heath Hill fault and the associated outcrops of Western Port Group and Older Volcanics; (2) Recharge in the west of the basin along the Tyabb monocline (e.g. where outcrops of the Baxter Formation are found); (3) Recharge of surface runoff into the Older Volcanics at outcrops east of the Heath Hill Fault, and subsequent upward flow into the Western Port Group; (4) Leakage of water from streams where Cainozoic sediments are overlain by permeable material; (5) Recharge of the Cainozoic sediments on French Island, which is a local topographic high. The Western Port Group occurs continuously below French Island and Western Port Bay, probably connecting with the onshore sediments to the north (Lakey and Tickell 1980). The distribution of radiocarbon and tritium activities support the first and second mechanisms of recharge; the highest tracer activities are found in shallow bores on the western margin near the Tyabb Monocline (91076) and the eastern margin, near Heath Hill (107475). While these are the youngest groundwater sampled, the still relatively low tritium concentrations (0.23 and 0.08 TU, respectively) and radiocarbon activities (73.2 and 78.8 pMC, respectively) indicate either that decades have elapsed since the water was recharged, or (more likely), that the modern component of water at these localities is diluted by a component of tracer-free water. The relatively high radiocarbon activities observed in samples collected along transect 2, near the Heath Hill Fault (Fig. 6), and relatively fresh salinities in this area support the notion that this is a major regional recharge area for the basin. Other recharge mechanisms (e.g. 3, 4 and 5) are difficult to substantiate without a wider spatial coverage of samples; however, the notion that under natural conditions groundwater in the Western Port Group was recharged by upward leakage from the Older Volcanics, is not well supported by the trend of declining radiocarbon activities with depth.

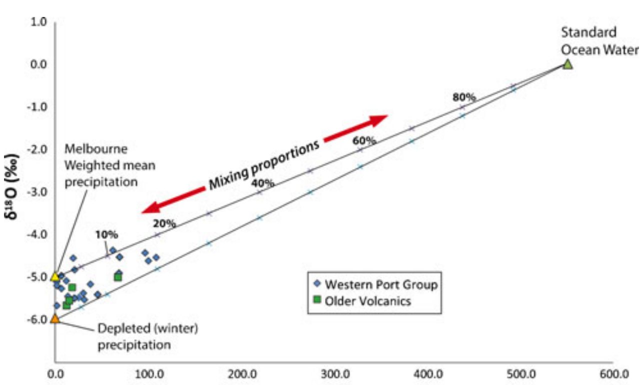


**Fig. 8** Chloride and $\delta^{18}O$ in groundwater, showing samples bracketed by mixing lines between standard ocean water and precipitation, with $\delta^{18}O$ between −5.0 and −6.0 ‰

A major complication in interpreting the age data is that 60 years of pumping has significantly changed the groundwater flow regime—with a reversal of the vertical gradients from upwards to downwards, and changes in the direction and magnitude of horizontal hydraulic gradients around the cone of depression. The degree of 'over-printing' of the pre-development distribution of groundwater ages is difficult to estimate—but the contrasting pattern of radiocarbon activities along transect 1, which includes the zone of pumping and transect 2 which does not, indicates that this effect is probably significant (Fig. 6). Apart from an obvious increase in estimated ages away from the recharge areas, there is little lateral variation in the estimated groundwater ages in the Older Volcanics or Western Port Group in the main zone of pumping (along transect 1); tracer concentrations within a given depth interval are mostly similar. Of particular note is the similarity in the $^{14}C$ values in the top ~50 m of the Western Port group in this area (e.g. samples with 21–23 pMC). One explanation is that pumping has facilitated a high level of mixing and dispersion, homogenizing the age distributions; another is that a common process, such as the oxidation of organic matter in the aquifer, results in similar $^{14}C$ values in this horizon. At this stage it is difficult to distinguish these mechanisms clearly, although the mostly homogeneous salinity values that are observed in the main zone of pumping (Cheng 1999) probably support the first explanation, relating to a large degree of mixing and solute dispersion. The low $^{14}C$ values in the Older Volcanics in comparison to the Western Port Group indicate that mixing

 DOI 10.1007/s10040-013-1017-9

between these two units is not extensive, possibly due to the presence of volcanic clay layers between them. A further interpretation of the zonation of radiocarbon activities that cannot be ruled out is that there may be a distinct zone or 'window' (spatially or temporally), through which recharge mainly occurred in each of the units (e.g. Meredith et al. 2012), which is preserved in the aquifer.

Based on the tracer data, flow rates for water following regional flow paths in the Western Port Group appear to be somewhat slower than previously proposed. For example, Carrillo-Rivera (1975) estimated water in the Western Port Group was flowing at ~0.2 km/year towards the centre of the cone of depression—under such a scenario, some water containing tritium might be expected to be found within ~10 km of the basin margins and this is not observed. Dilution of 'young water' drawn to the cone of depression by mixing with older water during transit may however mask its arrival.

## Water balance and response to pumping

The most noticeable features of groundwater hydrographs in the zone of pumping are the yearly decline and recovery of water levels, on the order of 2–4 m, and the general stability of aquifer pressures since the beginning of records (Fig. 9). It is important to note that there was an overall decline in the potentiometric head following major development of the resource in the 1950s and 1960s; prior to this the aquifer pressures were strongly artesian (Threader 1952). However, after 1970, when management policies limited extractions, the seasonal recovered pressures have remained generally constant until the present. Some variation in aquifer pressures appears to be attributable to trends in rainfall (Fig. 9). This may be partially due to greater recharge during wet years and/or a loading effect on confined aquifer layers; however, it probably mostly relates to the increased reliance on groundwater pumping during periods of low rainfall–drought periods strongly correspond to high rates of groundwater usage (Southern Rural Water 2010). Overall, the general stability in aquifer pressures since ca. 1970 indicates that the system has arrived at a new dynamic equilibrium since the early development of the resource.

A generalised water balance for the zone of groundwater extraction can be estimated on the basis of the approximate extent and size of the aquifer layers, water-level changes, and estimated storage coefficients from pumping tests conducted in the 1970s (e.g. Carrillo-Rivera 1975; Lakey and Tickell 1980). A decline in potentiometric head of ~3 m in a season, over an area of 15 km × 25 km, with an average storage coefficient of $5\times10^{-3}$ would give the total yearly water taken from storage in the Western Port Group to be approximately 5.5 GL; and in the Older Volcanics (which has a lesser lateral extent) ~2.25 GL. These estimates are similar, although slightly lower than those of Carrillo-Rivera (1975), and are close to the yearly pumpage rates estimated by Southern Rural Water (2010), combining licensed and unmetered extractions. Note that the storage coefficients used (Fig. 3) are at the high end of estimates derived from pumping tests and that replenishment via horizontal or vertical transfer

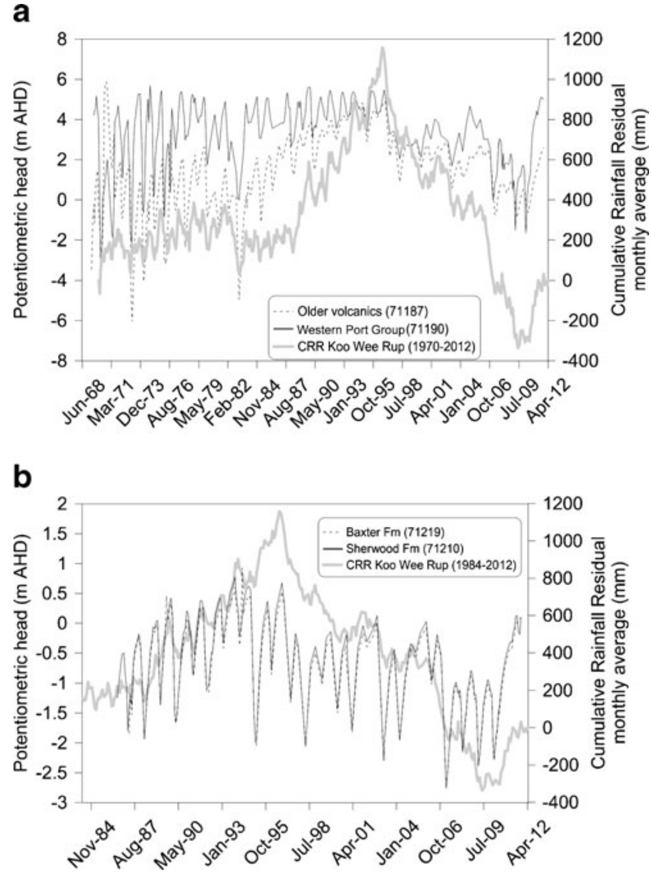


**Fig. 9** Hydrographs for two nested bore sites (locations shown in Fig. 1), showing reduced water level relative to the Australian Height Datum and cumulative rainfall residual (cumulative sum of the deviation of monthly rainfall totals from the long-term mean). **a** Bores *71187* and *71190* with cumulative rainfall residual, between 1970 and 2012; **b** nested bores *71219* and *71210* with cumulative rainfall residual, between 1984 and 2012. The groundwater from all of these bores contains no measurable tritium and has radiocarbon activities between of 3 and 22 pMC

during the pumping season may also be substantial. Assuming that on average an approximately constant volume has been extracted since the 1960s, the total amount of water pumped accounts for approximately $4.5\times10^{8}$ $m^3$, or ~8.5 % of the total storage capacity within the area affected by pumping. This includes both recoverable and unrecoverable storage in the Western Port Group and Older Volcanics. This estimate assumes a mean thickness of 50 m for the Western Port group and 30 m for the Older Volcanics in the main pumping area, and an average porosity of 0.2 (Lakey and Tickell 1980; Cheng 1999).

Given that aquifer pressures have generally exhibited recovery each season and that there has been overall stability of pressures since ca. 1970, the aquifer units within the zone of pumping must derive water from increased capture compared with the pre-development period, in accordance with (1) (Bredehoft 2002; Huang et al. 2012):

$$(R_0 + \Delta R) - (D_0 + \Delta D) + \Delta S = \mathrm{Pu} \qquad (1)$$

where, $R_0$=pre-development recharge, $D_0$=pre-development discharge, $S$=storage, Pu=pumpage.

 DOI 10.1007/s10040-013-1017-9

The additional capture could be derived from:

- A decrease in overall discharge from the basin (e.g. via artesian flow to the 'Great Swamp' that existed prior to development, or into the tidal channel of the bay).
- An increase in 'recharge' from other sources—such as leakage from units underlying or overlying the pumped layers, or horizontal transfer of water from further afield (e.g. from the offshore or eastern portions of the basin, where there are few extraction bores).
- Storage release by elastic and inelastic compressibility. Little evidence of any land subsidence (inelastic compressibility) in the region associated with pumping from the Western Port Group or Older Volcanics is documented.

The arrival of water at the pumping zone from undeveloped areas should be considered as part of the overall basin's water balance, and may manifest as a change in storage and/or declining pressures in parts of the basin outside the zone of pumping. This is distinct from a change in the overall basin recharge, which may increase due to greater surface-water leakage, or inter-basin flow from adjacent regions (at this stage there is insufficient evidence to assess or quantify these sources).

The low radiocarbon activities and almost complete lack of tritium in most groundwater indicate that very little water arriving at the zone of groundwater pumping during the recovery periods is derived from rapid arrival of recent recharge (e.g. the last 50 years). Most of the water is therefore from older (i.e. tracer-free) water sources such as leakage from low permeability layers, or lateral flow from more distant areas of the Western Port Group. There may for example be extensive stores of fresh groundwater in the offshore area below Western Port Bay, including French Island, and to the east, near Lang Lang from which water gradually migrates towards the zone of pumping, replenishing pumped water. Aquifer diffusivity in the horizontal and vertical dimensions will control the source(s) of water arriving at the zone of pumping (e.g. horizontal transfer versus vertical leakage).

## Sources of salinity

Groundwater salinities are generally highest in bores close to the coast of Western Port Bay (Fig. 10), and are higher in the shallower Baxter Formation than deeper layers. Groundwater is also generally more saline in coastal areas surrounding Tooradin (e.g. bore 71219) compared with regions further to the east or west—although a local patch of saline water approaching oceanic salinities also exists at Warneet. The major ion compositions (e.g., molar Cl/Br ratios between 652 and 1003) and stable isotope data (Figs. 7 and 8), suggest a marine source of solutes in much of the coastal groundwater. If evaporative concentration of soil water and subsequent recharge to groundwater was a dominant salinization mechanism, then far greater increases in $\delta^{18}O$ for a given increase in Cl would be expected to be observed (e.g. Clark and Fritz 1997). If salinization by transpiration and solute exclusion by

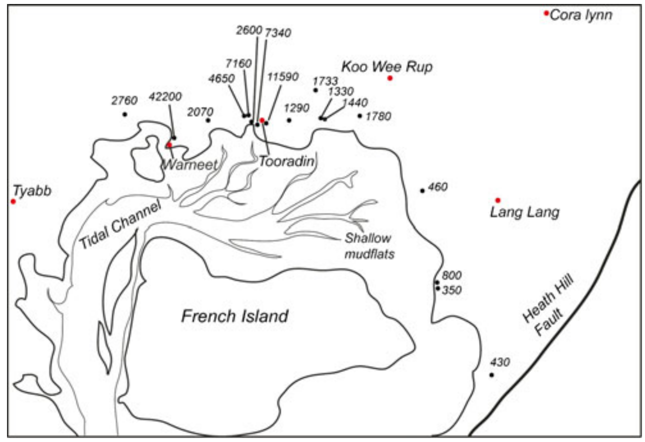


**Fig. 10** Distribution of groundwater salinity, as electrical conductivity (μS/cm) for monitored coastal bores in the Western Port Group in June 2011, and location of the tidal channel in Western Port Bay. *Black dots* are bores, *red* dots are towns

plants was an important process, as in the semi-arid Murray Basin of southeast Australia, then little change from the meteoric stable isotope compositions would be observed across the range of salinities sampled (Herczeg et al. 2001). Using conservative mixing calculations based on Cl and $\delta^{18}O$, the most saline groundwater (e.g. bore 71219) can be explained as a mixture of approximately 80–20 % rainfall/fresh groundwater to standard seawater (Millero 1996). Some evapotranspiration during recharge likely raises all groundwater salinities to Cl concentrations above those in rainfall; the freshest groundwater samples, from bores 145259 and 74609 contain approximately 2 mmol/L of Cl. Replacing the rainfall end-member with the freshest groundwater sample (1.8 mmol/L Cl and $\delta^{18}O$ of −5.1 ‰), results in only a negligible change in the estimated mixing proportions (less than 0.5 % for most samples), compared to when rainfall is used as the fresh end-member. Still, given that groundwater in semi-arid Australian environments typically undergoes some salinization due to ET, the 20 % marine component should be viewed as a maximum estimate of the seawater contribution to salinity. The mixing proportions (Fig. 8) are broadly consistent with stable isotope-chloride relationships observed by Cheng (1999), who calculated the proportion of marine water in coastal bores to be between 5 and 15 %.

The geological and geomorphological structure of the Western Port Basin precludes standard mechanisms of saline intrusion (Lakey and Tickell 1980). This is because Western Port Bay is shallow, with an average ocean floor depth of > −5 m AHD, and is mostly underlain by low permeability Quaternary clays and silts. Hence, in the majority of the bay there is no direct pathway for seawater to enter the Western Port Group. The only area where permeable material is intersected in the bay is the tidal channel, which reaches a depth of ~30 m in some regions. It was previously proposed by Lakey and Tickell (1980) that migration of saline water into the onshore portion of the Western Port Group occurs, but the amount and rate is constrained by permeability of bay floor sediments. Under

 DOI 10.1007/s10040-013-1017-9

their conceptual model, seawater leaks through the bay floor clays into the more permeable calcareous layer of the Sherwood Formation, and is drawn onshore under the gradients created by pumping. This water then mixes with fresh water in the sediments recharged at outcrops of the Western Port Group (e.g. on French Island and near Tyabb). A modified version of this conceptual model incorporating the data from this study is shown in Fig. 11. The model shows conceptually the sources of water at the coast of Western Port Bay, during the pre-development (pre 1950s) and post-development periods.

The geochemical data collected in this study is broadly consistent with the Lakey and Tickell model, but with some important differences. Firstly, water reaching the onshore part of the basin from the southwest (whether fresh or saline) is free of tritium and contains low radiocarbon activities, and therefore the rate of migration to this area from offshore is very gradual. The marine water component has only had a minimal effect on the groundwater-age-tracer activities—probably increasing the radiocarbon activity slightly above the 'pre-leakage' scenario, but not resulting in any measurable tritium in the samples affected by seawater. Also, the higher salinities observed in groundwater from the shallower parts of the Western Port Group (Baxter Formation), compared to deeper groundwater (Sherwood) indicate that a greater amount of marine leakage reaches these shallower sediments in the localities observed. This contrasts somewhat with the Lakey and Tickell model, which was focussed more on marine leakage into deeper sediments (below 30 m depth), particularly on the western side of the bay. The findings regarding saltwater/freshwater relationships in this study are consistent with solute transport modelling conducted by Cheng (1999), who simulated movement of fresh, brackish and saline water under changes in potentiometric pressures from the pre-development period, up until 1995.

### Temporal and spatial trends in water quality

The heterogeneous spatial distribution of groundwater salinities, particularly around the coast of Western Port Bay, including the more saline water occurring near Tooradin (Fig. 11) may be explained by one or more of the following:

- The influence of the spatially concentrated groundwater pumping causing higher fluxes of marine water from the bay to migrate to particular areas.
- The presence of preferential pathways—such as a more developed/incised tidal channel in the bay and/or occurrence of permeable sedimentary horizons providing an easier conduit for marine-water migration into certain areas of the aquifer.
- The influence of prior marine intrusion(s) during higher sea-level conditions (e.g. during the previous Holocene peak at ~6 ka, cf. Belperio et al 2002); and the subsequent degree of flushing of solutes by fresh water

As discussed in the preceding, there are areas around the coast (e.g. around Tooradin), where the recent intrusion of some marine water, probably under the influence of pumping, is evident. Areas of greater salinity broadly coincide with the location of the incised tidal channel near the coast, which deepens from east to west (Fig. 10). More regionally, the overall lower salinities and higher radiocarbon activities in the east of the basin compared to the central and western areas indicate that the degree of flushing of solutes is a major influence on current groundwater salinities in the basin. The greater level of flushing in the east can be explained by the greater topographic gradients and closer proximity to the Heath Hill fault, which appears to be a major recharge zone. As with the water-level observations, the recent stability in water quality (since ca. 1985) may represent the basin coming to a new 'equilibrium' or steady

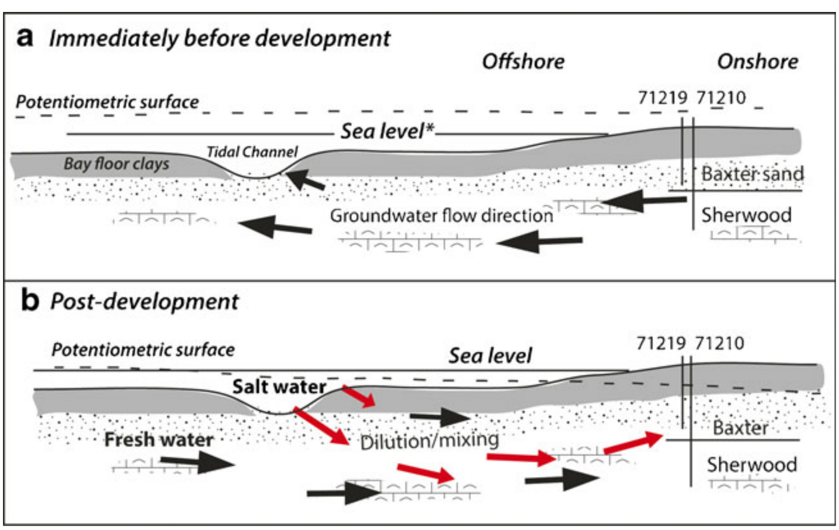


**Fig. 11** Conceptual model of the salinization mechanism for coastal groundwater bores near Tooradin, **a** before and **b** following development of the aquifer. For much of the period during which the groundwater was recharged, sea level would have been significantly lower, and Western Port Bay would have been largely exposed above sea level, potentially facilitating greater recharge in the French Island region. Modified from Lakey and Tickell (1980)


DOI 10.1007/s10040-013-1017-9

state with respect to sources of water and solutes, following an initial increase in salinities in the 1960s and 1970s as the system adjusted to stresses from extraction. While there is no major temporal trend observed in the average groundwater salinities since ca. 1985 (over multi-year timescales), there is fluctuation in salinities occurring over yearly/monthly timescales (Fig. 4). This can be understood as reflecting variable mixtures of fresher and more saline components of water arriving at the wells due to seasonal changes in hydraulic gradients and sources of water; namely the marine component, a fresh groundwater component, and any water released from storage in local low-permeability layers. The numerous clay inter-beds present in the Sherwood and Baxter Sand likely contain water with relatively low tracer activities and higher salinity, which may be released slowly in response to draining of more permeable layers; while the more permeable horizons may act as local conduits for fresher water arriving from other parts of the basin during non-pumping periods. Tidal effects may also be important, in terms of their control on hydraulic gradients at the coast. There are a large number of overlapping mechanisms that control pore-water advection in coastal areas; Santos et al. (2012) recently described twelve separate mechanisms driving flow of coastal pore waters. This means that it is difficult to define and quantify the processes controlling cyclical salinity fluctuations in this and other similar aquifers with precision. However, given the confined nature of the aquifer, the seasonal changes in aquifer levels on land are likely to be an important driver of flow at the coast in this system. Future work will aim to examine these effects in more detail.

### Management implications

The relatively long groundwater residence times, and the generally slow process of incorporation and dilution of recharge into the basin (as opposed to a system in which rapid cyclical recharge and flushing occurs), has important management implications. In particular, any adverse water-quality impacts such as salinization affecting the aquifer units may take some time to reverse. At the same time, the large storage and dilution capacity mean that water-quality changes are likely to be attenuated and take a long time to manifest. This is unless such changes occur as localized effects, for example, due to preferential flow paths. Integrated groundwater-management strategies such as managed aquifer recharge, must also be mindful of the limited rates of modern recharge and relatively slow travel times in the basin. At present, there is little evidence of adverse water-quality impacts arising due to mechanisms such as bore failure and rapid leakage of agricultural runoff from the surface to the water-supply aquifers—if these were occurring then tritium, and compounds related to surface agriculture such as nitrate would be expected to be found at depth. While there are local areas of higher salinity water located near Tooradin and Warneet, there has generally not been a major increase in groundwater salinities or spread of saline water to other parts of the basin since regular water-quality monitoring began in the mid-1980s, as was initially feared following intensive development of the basin.

The previously proposed conceptual model of leakage and incorporation of marine water into the onshore portion of the basin, under the influence of landward hydraulic gradients, is broadly consistent with the data collected in this study, but this occurs on longer timescales than previously described (e.g. Lakey and Tickell 1980). The radioisotope data indicate that while transmission of water from the offshore part of the basin to the onshore region is potentially important, the water reaching the pumping zone in response to drawdown is still ‘old’ water. Thus, water that recharges in the French Island/Tyabb region and on the eastern and western margins, will still take a long time to reach the zone of pumping, and it is likely that little or none of this water has yet reached the onshore part of the basin since development of the aquifer for irrigation supply. Protection of water quality in these areas is therefore an important long-term management goal, as changes in the quality of recharge may still take some time to manifest in the pumping/water-supply area.

## Conclusions

Key findings from this study can be summarized as follows:

1. Groundwater in much of the Western Port Basin aquifer contains no detectable tritium, indicating that any water recharged since widespread development of the aquifer (in the early 1960s) makes up only a small component of the water currently in the basin. Low radiocarbon activities in the main aquifer units also indicate much of the groundwater was recharged in pre-modern times, during the early Holocene and late Pleistocene.
2. Recharge of groundwater at the eastern and western margins of the basin—the Heath Hill Fault and Tyabb Monocline is supported by the presence of water containing tritium and relatively high radiocarbon activities.
3. In zone of pumping, the aquifer has reached a condition where potentiometric pressures recover seasonally, and have not declined substantially since the early 1970s. The additional capture facilitating seasonal recovery is probably the transfer of water from distant, undeveloped areas and/or release of water from storage in low permeability layers. Very little if any modern water has arrived at the zone of pumping since large-scale exploitation began, and the amount of water extracted since the early 1960s likely represents something on the order of ~8 % of total aquifer storage in the zone of pumping.
4. Seawater is the main source of solutes in the relatively saline groundwater located locally near the coast; this groundwater can be explained as a mixture of fresh recharge, and small components (maximum 20 %) of marine water.
5. The present-day spatial distribution of salinity has been influenced by heterogeneous hydraulic gradients, geological structure and the degree of solute flushing by

 DOI 10.1007/s10040-013-1017-9

fresh recharge. The fresher water consistently found in the east of the basin can be explained as a result of a greater degree of flushing by recharge entering at the Heath Hill Fault zone.

6. The lack of modern water in the zone of groundwater extraction, and the relatively long travel times required for water to move from recharge areas to reach the zone of extraction, mean that any changes in water quality in recharge areas will likely take a long time to manifest within the areas where groundwater is used for water supply. Management of land-use and groundwater extraction activities should therefore be mindful of the potential delay in the onset of such effects.

**Acknowledgements** The authors would like to thank AINSE Ltd for providing financial assistance (Award No. ALNGRA12007), to enable work on radio-isotope tracers to be conducted. Also, UNESCO IGCP-618 project (Palaeoclimate information obtained from past-recharged groundwater) is acknowledged for financial support. We thank Dr Ben Gilfedder, Mr Stephen Lee, Mr Ali Suleman and Mr Dan Perera for their assistance during field work, and Professor Ian Cartwright and Dr Massimo Raveggi for assisting in the analysis of stable isotopes and major ions.

## References

Alley WM, Reilly TE, Franke OL (1999) Sustainability of groundwater resources. US Geol Surv Circ 1186, 79 pp

Andersen MS, Jakobsen VNR, Postma D (2005) Geochemical processes and solute transport at the seawater/freshwater interface of a sandy aquifer. Geochim Cosmochim Acta 69:3979–3994

Barlow PM, Reichard EG (2010) Saltwater intrusion in coastal regions of North America. Hydrogeol J 18:247–260

Belperio AP, Harvey N, Bourman RP (2002) Spatial and temporal variability in the Holocene sea-level record of the South Australian coastline. Sed Geol 150:153–169

Bredehoeft J (2002) The water budget myth revisited: why hydrogeologists model. Ground Water 40:340–345

Calf GE (1988) Tritium activity in Australian rainwater 1962–1986. Aus Nucl Sci Tech Org Rep. E-680

Carrera J, Hidalgo JJ, Slooten LJ, Vázquez-Suñé E (2010) Computational and conceptual issues in the calibration of seawater intrusion models. Hydrogeol J 18:131–146

Carrillo-Rivera JJ (1975) Hydrogeology of Western Port. Geol Surv Victoria Rep 75/1

Cartwright I, Weaver TR, Simmons CT, Fifield LK, Lawrence CR, Chisari R, Varley S (2010) Physical hydrogeology and environmental isotopes to constrain the age, origins and stability of a low-salinity groundwater lens formed by periodic river recharge: Murray Basin, Australia. J Hydrol 380:203–221

Cheng X (1999) Impact of groundwater abstraction on groundwater flow and solute transport, Western Port Basin, Victoria. MSc Thesis, University of Melbourne, Australia, 358 pp

Clark I, Fritz P (1997) Environmental isotopes in hydrogeology. Lewis Publishing, New York, 328 p

Coetsiers M, Walraevens K (2009) A new correction model for 14C ages in aquifers with complex geochemistry: application to the Neogene Aquifer, Belgium. Appl Geochem 24:768–776

Fink D, Hotchkis M, Hua Q, Jacobsen G, Smith AM, Zoppi U, Child D, Mifsud C, van der Gaast H, Williams A, Williams M (2004) The ANTARES AMS facility at ANSTO. Nucl Instr Meth Phys Res (B) 223–224:109–115

Fontes J-C, Garnier J-M (1979) Determination of the initial $^{14}C$ activity of the total dissolved carbon: a review of the existing models and a new approach. Water Res Res 15: 399–413

Gattacceca JC, Vallet-Coulomb C, Mayer A, Claude C, Radakovitch O, Conchetto E, Hamelin B (2009) Isotopic and geochemical characterisation of salinization in the shallow aquifers of a reclaimed subsiding zone: the southern Venice Lagoon coastland. J Hydrol 378:46–61

Gillon M, Barbecot F, Gibert E, Corcho Alvarado JA, Marlin C, Massault M (2009) Open to closed system transition traced through the TDIC isotopic signature at the aquifer recharge stage, implications for groundwater 14C dating. Geochim Cosmochim Acta 73:6488–6501

Han L-F, Plummer LN, Aggarwal P (2012) A graphical method to evaluate predominant geochemical processes occurring in groundwater systems for radiocarbon dating. Chem Geol 318–319:88–112

Herczeg AL, Edmunds WM (2000) Inorganic ions as tracers. In: Herczeg AL, Cook P (eds) Environmental tracers in subsurface hydrology. Kluwer, Dordrecht, The Netherlands

Herczeg AL, Dogramaci SS, Leaney FWJ (2001) Origin of dissolved salts in a large, semi-arid groundwater system: Murray Basin, Australia. Mar Freshw Res 52:41–52

Huang Y, Scanlon BR, Nicot J-P, Reedy RC, Dutton AR, Kelley VA, Deeds NE (2012) Sources of groundwater pumpage in a layered aquifer system in the Upper Gulf Coastal Plain, USA. Hydrogeol J 20:783–796

Hughes CE, Crawford J (2012) A new precipitation weighted method for determining the meteoric water line for hydrological applications demonstrated using Australian and global GNIP data. J Hydrol 464–465:344–351

Jiráková H, Huneau F, Celle-Jeanton H, Hrkal Z, Le Coustumer P (2011) Insights into palaeorecharge conditions for European deep aquifers. Hydrogeol J 19:1545–1563

Lakey R, Tickell SJ (1980) Effects of channel dredging in Tyabb area on Western Port Basin Groundwater. Geol Surv Victoria Rep 58

Lakey R, Tickell SJ (1981) Explanatory notes on the Western Port Groundwater Basin 1:100000 hydrogeological map. Geol Surv Victoria Rep 69

Longley TS, Turner AK, Lawson JD (1978) Modelling aquifer recharge and water use in the Koo-Wee-Rup basin. Aus J Soil Res 16:245–256

Love AJ, Herczeg AL, Leaney FW, Stadter MF, Dighton JC, Armstrong D (1994) Groundwater residence time and palaeohydrology in the Otway Basin, South Australia: $^{2}H$, $^{18}O$ and $^{14}C$ data. J Hydrol 153:157–187

Meredith K, Cendón DI, Pigois J-P, Hollins S, Jacobsen G (2012) Using $^{14}C$ and $^{3}H$ to delineate a recharge 'window' into the Perth Basin aquifers, North Gnangara groundwater system, Western Australia. Sci Tot Env 414:456–469

Millero FJ (1996) Chemical oceanography. CRC, Boca Raton, FL

Morgentern U, Stewart MK, Stenger R (2010) Dating of streamwater using tritium in a post nuclear bomb pulse world: continuous variation of mean transit time with streamflow. Hydrol Earth Sys Sci 14:2289–2301

Mulligan AE, Evans RL, Lizarralde D (2007) The role of palaeochannels in groundwater/seawater exchange. J Hydrol 335:313–329

Parkhurst DL, Apello CAJ (1999) User's guide to PHREEQC (Version 2)—a computer program for speciation, batch-reaction, one-dimensional transport, and inverse geochemical calculations. USGS Water Resource Investigation Report 99–4259

Post V, Abarca E (2010) Preface: saltwater and freshwater interactions in coastal aquifers. Hydrogeol J 18:1–4

Rosengren NJ (1984) Sites of geological and geomorphological significance in the Western Port Bay catchment. Department of Conservation, Forests and Lands, Melbourne, 513 pp

Santos IR, Eyre BD, Huettel M (2012) The driving forces of porewater and groundwater flow in permeable coastal sediments: a review. Estuar Coast Shelf Sci 98:1–15

Sinclair Knight Merz (1997) Western Port groundwater monitoring review. Sinclair Knight Merz, Melbourne, 59 pp

Sinclair Knight Merz (2003) Koo Wee Rup water supply protection area technical assessment. Final report. Sinclair Knight Merz, Melbourne, 49 pp

Southern Rural Water (2010) Groundwater management plan, Koo Wee Rup water supply protection area. Southern Rural Water, Warrnambool, Australia, 25 pp

Strack ODL (1976) A single-potential solution for regional interface problems in coastal aquifers. Water Res Res 12:1165–1174

Stuiver M, Polach A (1977) Reporting of $^{14}C$ data. Radiocarbon 19:355–363

Threader VM (1952) Underground water resources, Bunyip River valley and the Mornington Peninsula. SRWSC Victoria Water Res Investigation Report, SRWSC, Eildon, Australia, 9 pp

Været L, Leijnse A, Cuamba F, Haldorsen S (2012) Holocene dynamics of the salt–fresh groundwater interface under a sand island, Inhaca, Mozambique. Quat Int 257:74–82

Vengosh A, Gill J, Davisson ML, Hudson B (2002) A multi-isotope (B, Sr, O, H and C) and age dating ($^{3}H$–$^{3}He$ and $^{14}C$) study of groundwater from Salinas Valley, California: hydrochemistry, dynamics and contamination processes. Water Res Res 38:WR000517

Vengosh A, Kloppmann W, Marei A, Livshitz Y, Gutierrez A, Banna M, Guerrot C, Pankratov I, Raanan H (2005) Sources of salinity and boron in the Gaza Strip: natural contaminant flow in the southern Mediterranean coastal aquifer. Water Res Res 41:W01013

Werner AD, Simmons CT (2009) Impact of sea-level rise on sea water intrusion in coastal aquifers. Ground Water 47:197–204

Werner AD, Ward JD, Morgan LK, Simmons CT, Robinson NI, Teubner MD (2012) Vulnerability indicators of sea water intrusion. Ground Water 50:48–58



DOI 10.1007/s10040-013-1017-9